



1 *Conference Proceedings Paper*

2 **Remote sensing of near real-time heavy precipitation** 3 **using observations from GPM and MFG over India** 4 **and nearby oceanic regions**

5 **Mohammd Rafiq* and Anoop Kumar Mishra**

6 Centre for Remote Sensing and Geoinformatics, Sathyabama, University Chennai, TN

7 * Correspondence: emidamls6@gmail.com; Tel.: +91-9469183781

8 Published: date

9 **Abstract:** This study deals with the integration of merging highly accurate precipitation estimates from
10 Global Precipitation Measurement (GPM) with sampling gap-free satellite observations from Meteosat 7 of
11 Meteosat First Generation (MFG) to develop a regional rainfall monitoring algorithm for monitoring
12 precipitation over India and nearby oceanic regions. For this purpose, we derived precipitation signatures
13 from Meteosat observations to co-locate it against precipitation from GPM. A relationship is then established
14 between rainfall and rainfall signature using observations from various rainy seasons. The relationship thus
15 derived can be used to monitor precipitation over India and nearby oceanic regions. Performance of this
16 technique was tested against rain gauges and global precipitation products including the Global Satellite
17 Mapping of Precipitation (GSMaP), Climate Prediction Centre MORPHing (CMORPH), Precipitation
18 Estimation from Remote Sensing Information using Artificial Neural Network (PERSIANN) and Integrated
19 Multi-satellitE Retrievals for GPM (IMERG). A case study is presented here to examine the performance of
20 the developed algorithm for monitoring heavy rainfall during flood event of Tamil Nadu in 2015. This is the
21 first attempt to use near real time observations from GPM and MFG to monitor heavy precipitation over
22 Indian region. Due to finer resolution and near real time availability, this technique can be used to monitor
23 near real time flash floods.

24 **Keywords:** Precipitation estimation; NRT precipitation; Flood; Drought; Convective Clouds
25

26 **1. Introduction**

27 Near Real Time NRT precipitation information at fine resolution is required to monitor flash
28 floods. Unfortunately Indian region have poor density of ground based rain gauges and Radars.
29 Moreover, usually rain gauge stations stop functioning during severe flood situations (Mishra,
30 2015). Flood events are associated with a large spatial and temporal variation of rainfall and hence
31 continuous NRT high resolution hourly satellite data is essential to monitor such events (Mishra and
32 Srinivasan, 2013). Such observations can be achieved by merging microwave precipitation estimates
33 with rain signatures from geostationary satellites. Past researches report that cold observations from
34 IR are associated with convective clouds and thus heavy precipitation (Mishra et al. 2010; Mishra
35 2013). In the past few decades, various satellite precipitation products have become widely available
36 for users. These data sets integrate precipitation estimates and signatures from different sensors and
37 satellites into a precipitation product. These data sets include the Tropical Rainfall Measuring
38 Mission Mission (TRMM) Multisatellite Precipitation Analysis (TMPA) NRT product (Huffman et al.,
39 2007), the Global Satellite Mapping of Precipitation (GSMaP) (Kubota et al., 2007; Aonashi et al., 2009),
40 Climate Prediction Centre MORPHing (CMORPH) (Joyce et al. 2004), Precipitation Estimation from
41 Remote Sensing Information using Artificial Neural Network (PERSIANN) (Hsu et al. 1997), Hydro-
42 Estimator (H-E) (Scofield and Kuligowski, 2003), and Integrated Multi-satellitE Retrievals for GPM
43 (IMERG) (Huffman et al. 2015). Validation results show that most of these products have large

44 errors over Indian region (Mishra et al. 2010; Mishra 2013). Mishra et al. (2009a) reported that regional
45 rain signatures derived for India outperform global rainfall signatures for their application over
46 India. Few efforts have been made to monitor rainfall over India and nearby region by synergistic
47 use of multi-satellite sensors (Mishra et al. 2009b, 2010; Mishra et al. 2011a, b; Mishra, 2012; Mishra,
48 2013). Availability of microwave measurements with broader swath and high frequency ice scattering
49 channels from GPM provide a unique opportunity to merge accurate microwave rainfall information
50 with Infrared observations from Meteosat over India. The GPM Core Observatory measures
51 precipitation using two sensors: the GPM Microwave Imager (GMI) and the Dual-frequency
52 Precipitation Radar (DPR). A recent preliminary study reports that rainfall estimates from DPR
53 onboard GPM are closer to the gauge estimates than those from PR onboard TRMM (Iguchi et al.
54 2009).

55 In this study, we have merged observations from combined DPR and GMI with Meteosat to
56 monitor near real time precipitation over Indian region and nearby ocean. Validations have been
57 performed using rain gauge based product to test the accuracy of the present approach for its
58 application in heavy rainfall cases.

59 2. Data used and study Area

60 For the present study, Meteosat 7 data of Meteosat First Generation (MFG) is used. MFG provides
61 images of the full Earth disc, and data for weather forecasts. Meteosat provides observations in
62 Thermal Infra Red (TIR) and Water Vapor (WV) absorption band at half-hourly interval, with a
63 spatial resolution of 4 km. Combined GMI-DPR based rainfall from GPM is also used in this study.
64 This product is described by Grecu et al., (2009; 2016). In order to test the performance of present
65 technique, rainfall estimates from GSMaP, CMORPH, PERSIANN and IMERG has also been used in
66 the present technique. Rain gauge observations from AWS is used to validate the performance of
67 present technique. Study area spans from 10°S-40°N to 60E°-100E°.

68 3. Methodology

69 Multi-frequency observations at multiple channels from Meteosat were used to filter out false
70 rainfall signatures. We used a cloud classification scheme devised by Roca et al. (2002) and adopted
71 by Mishra et al. (2010) to delineate non rainy thin cirrus clouds. If brightness temperature in IR band
72 (IRTB) $\geq 270\text{K}$ and cloudy and brightness temperature in WV band (WVTB) $\leq 246\text{K}$ then pixel
73 represents thin cirrus clouds and is screened out. During day time, cloud microphysical properties at
74 near IR observations and visible reflectance were used to screen in rainy pixels following criteria used
75 by Rosenfeld and Gutman (1994).

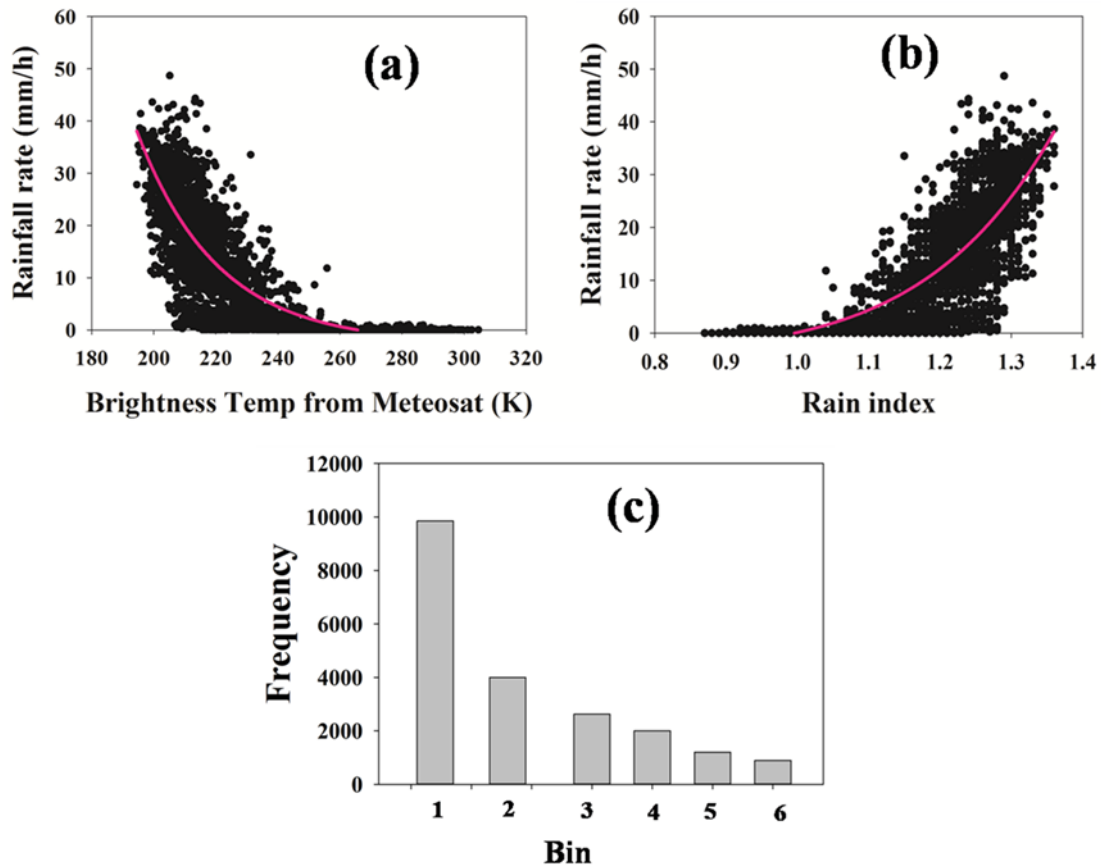
76 It was reported by Mishra et al. (2010) that few cirrus clouds were still undetected even after
77 applying threshold based cloud classification. In order to screen out the non rainy cirrus clouds, we
78 used a criteria developed by Adler and Negri (1988) as a second step. Following this approach, a slope
79 (S) and a temperature gradient (Gt) were estimated for each local temperature minimum (using
80 brightness temperature (IRTB) at 11.5 μm). The terms Gt and S are computed by Eq. (1) and Eq. (2),
81 respectively:

$$82 \quad Gt = IRTB_{avg} - IRTB_{min} \quad (1)$$

$$83 \quad S = 0.568(IRTB_{min} - 217) \quad (2)$$

84 Where IRTB_{min} is the local minimum, and as in Adler and Negri (1988), IRTB_{avg} is the mean
85 temperature. It may be noted that local minima is computed for an area covered by 6 IR pixels (4
86 pixels along the scan and 2 pixels across the scan). A large Gt shows convective clouds; a small
87 Gt represents a weak gradient and shows the presence of cirrus clouds within the window. All pixels
88 having Gt less than S are classified as cirrus clouds and therefore are rejected as non-raining clouds.

89 Following filtering out erroneous clouds, IRTB were co-located against combined GMI-DPR
 90 rainfall within 15 minutes of difference in which auto covariance function of rainfall reduces to about
 91 0.9 (Laughlin, 1981). "15 minutes of difference" is the maximum allowed time difference in
 92 simultaneous observations of GPM and Meteosat. Data re-sampling scheme is used to minimize the
 93 uncertainty in co-location due to difference in resolution. For the co-location process, rainfall from
 94 GPM is remapped at 0.1° grid. Now IR-Observations from Meteosat is also remapped at 0.1° grid. Co-
 95 location process is similar as described in Mishra et al. (2010). It may be noted that present algorithm
 96 aims to estimate rainfall at 0.1° grid.



97
 98 **Figure 1.** Scatter plot between rainfall rate (from GPM) and (a) brightness temperature (from
 99 Meteosat) (b) and rain index. (c) Histogram of frequency at different bins. Precipitation bins are
 100 defined as 2 mm/h, 8 mm/h, 15 mm/h, 20 mm/h, 25 mm/h and 30 mm/h (Selected Bin sizes set to
 101 accommodate the entire rainfall spectrum). Figure Source (Mishra and Rafiq 2017, Dynamics of
 102 Atmospheres and oceans).

103 For the co-location purpose, 18654 data points (re-sampled at 0.1° grid) consisting of rain events
 104 during the years 2015 and 2016 were used. Out of 18654 data points, 6642 were rainy pixels while
 105 12012 were no rainy pixels. A total number of 12862 were used for the independent validation
 106 purpose. This shows that out of 31515 (18654+12862) data points 41% of total data points were used
 107 for the validation purpose.

108 Relationship between IRTB and rainfall is shown in figure 1a. It can be seen that heavy rainfall
 109 events are associated with cold brightness temperature representing convective and deep convective
 110 clouds. Good correlation between rainfall and IRTB may be attributed to the inclusion of good
 111 number of heavy rainfall events (convective) and delineation of erroneous cirrus clouds.

112 A non rainy threshold of about 264K (IRTB0) is observed. We define rain index (RI) as follows:

113
$$RI = (IRTB_0 / IRTB) \quad (3)$$

114 IRTB>264K indicates RI<1 and is a representative of non rainy cases. Higher values of RI shows
115 heavy rainfall associated with intense rainy systems. RIs thus estimated are collocated against GMI-
116 DPR rainfall to establish a regression equation between them (figure 1b). We have classified the
117 precipitation spectrum (and corresponding brightness temperature and rain index) into 6 bins. These
118 precipitation bins are defined as 2 mm/h, 8 mm/h, 15 mm/h, 20 mm/h, 25 mm/h and 30 mm/h. Figure
119 1c shows that histogram of number of occurrences of these bins.

120 It can be seen from figure 1b that there are large scatters between rainfall and rain index which
121 is attributed to various factors ranging from uncertainty caused by use of different sensors from
122 different platforms (difference in viewing geometry from MFG and GPM), collocation errors, poor
123 relationship between warm rain (light rain) and IR brightness temperature, and weak
124 characterization of orographic rain from IR signature.

125 Following equation is established between RI and rain rate:

$$126 \text{ Rain rate (mm/h)} = a + (b \times \text{RI}^c) \quad (4)$$

127 Where $a = -3.79$ (mm/h),

128 $b = 4.55$ (mm/h), and

129 $c = 6.68$.

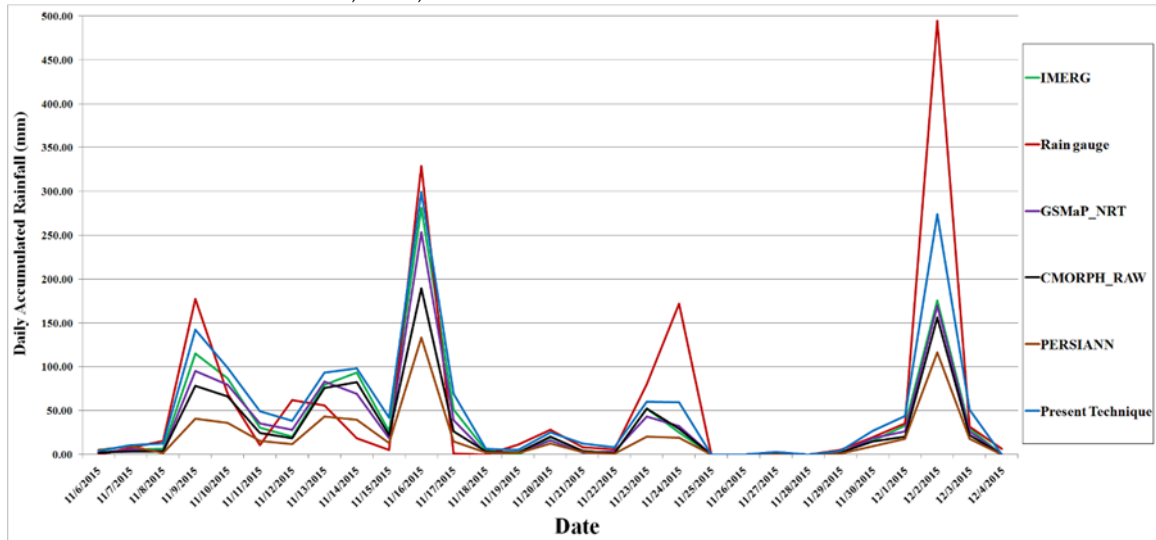
130 Coefficients 'a' and 'b' essentially characterize the relationship between rain rate and rain index,
131 allowing for variation caused by scatter in rain rate and rain index. This relationship exhibits a
132 Correlation Coefficients (CC) of 0.83, and Standard error of estimates of 6.20 mm/h. This relationship
133 confirms the power law relationship between rain index and rainfall as observed by past researches
134 (Mishra et al., 2009a; Mishra 2013). RI ranges from 0.86 to 1.37. It can be concluded from figure 1b that
135 RI>1.3 indicates heavy rainfall cases 25 mm/h and above (observation of line of fit indicated by pink
136 color in figure 1b). 4. Discussion

137 This section may be divided by subheadings. Authors should discuss the results and how they
138 can be interpreted in perspective of previous studies and of the working hypotheses. The findings
139 and their implications should be discussed in the broadest context possible. Future research
140 directions may also be highlighted.

141 4. Results and Discussion

142 Aim of the present algorithm is to monitor near real time heavy rainy systems. Performance of
143 this technique was tested by applying it to few flood events. We have used rain gauge observation
144 over Tamil Nadu for validation of present algorithm during flood event of Tamil Nadu in 2015.

145 Tamil Nadu witnessed heavy flooding during November- December in 2015. A case study has
146 been performed for Tambram region (12.933°N, 80.216°E) of Kancheepuram district in Tamil Nadu
147 during the severe flood events of 2015. For this purpose daily rainfall data from regional
148 meteorological centre, Chennai has been used. Rain gauge based daily rainfall is estimated by
149 accumulating rainfall in 24 hours ending 08:30 IST (03:00 GMT). For this validation purpose, hourly
150 rainfall from IMERG, GSMaP_NRT, CMORPH_RAW, PERSIANN is accumulated in starting at 03:00
151 GMT of the previous day to 03:00 GMT of the day named.



152

153

154

Figure 2. Rainfall over Tambram from Rain gauge, IMERG, GSMaP, CMORPH, PERSIANN and present technique during floods of 2015.

155

156

It can be seen that satellite estimates underestimate heavy rainfall. Among satellite estimates, present technique is closest to rain gauge observations for monitoring heavy rainfall.

157

5. Conclusions

158

159

160

161

162

163

164

165

166

167

168

169

170

171

172

173

Present study merges rainfall information from combined GMI-DPR with Meteosat observations by using the high accuracy of GMI-DPR based rainfall estimates and continuous Meteosat observations to monitor heavy precipitation. It offers an opportunity to explore the climatic aspect of heavy precipitation at finer scale since MFG has long past records. Studies suggest that being able to monitor extreme rainfall at finer resolution would be sufficient to monitor flash flood (Mishra and Srinivasan 2013; Mishra 2015). Present algorithm monitors near real time heavy rainfall which is very crucial for near real time flash flood monitoring. Mishra and Rafiq (2017) used this technique to study heavy precipitation over Indian region during active phase of South West Monsoon season. This is the first attempt to monitor near real time heavy precipitation over India by synergistic use of multisatellite sensors from GPM and MFG. Past researches report that heavy precipitation events over Indian region have been changed as a result of warming (Goswami et al. 2006; Mishra and Liu 2014). These heavy precipitation causes flood like disasters. Recently various parts of Indian region experienced flood like events (Mishra and Srinivasan 2013; Mishra 2015; Mishra 2016; Rafiq and Mishra 2017). Present technique can be very useful to monitor near real time flash flood events which can be helpful for mitigation and adaptation actions against flood related disasters.

174

175

176

Acknowledgments: All sources of funding of the study should be disclosed. Please clearly indicate grants that you have received in support of your research work. Clearly state if you received funds for covering the costs to publish in open access.

177

178

Conflicts of Interest: We acknowledge the funding for this work from ISRO under grant No. B. 19012/174/2016-Sec.2. Meteosat data from EUMETSAT and GPM data used in this study is also thankfully acknowledged.

179

References

180

181

182

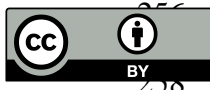
183

184

1. Adler, R. F. and Negri, A. J., 1988: A satellite infrared technique to estimate tropical convective and stratiform rainfall. *Journal of Applied Meteorology*, 27(1), 30–51.
2. Aonashi, K.; Awaka, J.; Hirose, M.; Kozu, T.; Kubota, T.; Liu, G.; Shige, S.; Kida, S.; Seto, S.; Takahashi, N. and Takayabu, Y. N. 2010: GSMaP passive microwave precipitation retrieval algorithm: Algorithm description and validation. *J. Meteorol. Soc. of Japan*, 87A, 119–136. doi:10.2151/jmsj.87A.119.

- 185 3. Goswami, B.N.; Venugopal, V.; Sengupta, D.; Madhusoodanan, M.S. and Xavier, P.K. 2006: Increasing
186 trend of extreme rain events over India in a warming environment. *Science*, 314(5804), pp.1442-1445.
- 187 4. Grecu, M.; Olson, W.S.; Munchak, S.J.; Ringerud, S.; Liao, L.; Haddad, Z.; Kelley, B.L. and McLaughlin, S.F.
188 2016: The GPM Combined Algorithm. *Journal of Atmospheric and Oceanic Technology*, 33(10), pp.2225–
189 2245.
- 190 5. Grecu, M.; Olson, W. S.; Shie, C. L.; L’Ecuyer, T. S. and Tao, W. K. 2009: Combining Satellite Microwave
191 Radiometer and Radar observations to estimate atmospheric heating profiles. *Journal of Climate*,
192 22(23),6356–6376.
- 193 6. Huffman, G. J.; Adler, R. F.; Bolvin, D. T.; Gu, G.; Nelkin, E. J.; Bowman, K. P.; Hong, Y.; Stocker, E. F. and
194 Wolff, D. B. 2007: The TRMM Multisatellite Precipitation Analysis (TMPA): Quasi-global, multiyear,
195 combined-sensor precipitation estimates at fine scales. *J. Hydrometeorol*, 8, 38–55. doi:10.1175/JHM560.1.
- 196 7. Huffman, G. J. and coauthors 2015: NASA Global Precipitation Measurement (GPM) Integrated Multi-
197 satellitE Retrievals for GPM (IMERG), Algorithm Theoretical Basis Document (ATBD) Version 4.5, NASA,
198 https://pmm.nasa.gov/sites/default/files/document_files/IMERG_ATBD_V4.5_0.pdf.
- 199 8. Iguchi, T.; Kozu, T.; Kwiatkowski, J.; Meneghini, R.; Awaka, J., and Okamoto, K. I., 2009: Uncertainties in
200 the Rain Profiling Algorithm for the TRMM Precipitation Radar. *Journal of the Meteorological Society of*
201 *Japan*, 87, 1–30.
- 202 9. Joyce, R. J.; Janowiak, J. E.; Arkin, P. A. and Xie, P. 2004: CMORPH: A method that produces global
203 precipitation estimates from passive microwave and infrared data at high spatial and temporal resolution.
204 *J. Hydromet*, 5, 487–503.
- 205 10. Kubota, T.; Shige, S.; Hashizume, H.; Aonashi, A.; Takahashi, N.; Seto, S.; Hirose, M.; Takayabu, Y. N.;
206 Ushio, T.; Nakagawa, K.; Iwanami, K.; Kachi, M. and Okamoto, K.. 2007: Global precipitation map using
207 satellite-borne microwave radiometers by the GSMaP project: Production and validation. *IEEE T. Geosci.*
208 *Remote*, 45, 2259–2275.
- 209 11. Laughlin, C. R. 1981: On the effect of temporal sampling on the observation of mean rainfall, *Precipitation*
210 *measurements from space*. Work-shop report, edited by D. Atlas and O. W. Thiele, pp. D59–D66, NASA /
211 Goddard Space Flight Cent., Greenbelt, Md.
- 212 12. Mishra, A. 2012: Estimation of heavy rainfall during cyclonic storms from microwave observations using
213 nonlinear approach over Indian Ocean. *Natural Hazards*, 63, 673-683. DOI 10.1007/s1 1069-012-0179-4.
- 214 13. Mishra, A. 2013: A new technique to estimate precipitation at fine scale using multifrequency satellite
215 observations over Indian land and oceanic regions. *IEEE Transactions on Geoscience and Remote*
216 *Sensing*,51(7), 4349–4358.
- 217 14. Mishra, A. 2015: A study on the occurrence of flood events over Jammu and Kashmir during September
218 2014 using satellite remote sensing. *Natural Hazards*, 78, 1463–1467.
- 219 15. Mishra, A.K. 2016: Monitoring Tamil Nadu flood of 2015 using satellite remote sensing. *Natural Hazards*,
220 82(2), pp.1431-1434.
- 221 16. Mishra, A. and Srinivasan, J. 2013: Did a cloud burst occur in Kedarnath during 16 and 17 June 2013.
222 *Current Science*, 105(10),1351–1352.
- 223 17. Mishra, A.; Gairola, R. M. and Agarwal, V. K. 2011a: Rainfall Estimation from combined observations using
224 KALPAANA-IR and TRMM-Precipitation Radar measurements over Indian Region. *Journal of Indian*
225 *Society of Remote Sensing*, 40(1), 65–74.
- 226 18. Mishra, A. and Liu, S.C. 2014: Changes in precipitation pattern and risk of drought over India in the context
227 of global warming. *Journal of Geophysical Research: Atmospheres*, 119(13), pp.7833–7841.
- 228 19. Mishra, A.; Gairola, R. M.; Varma, A. K. and Agarwal, V. K. 2009b: Study of Intense Heavy Rainfall Events
229 over India Using KALPANA-IR and TRMM- Precipitation Radar Observations. *Current Science*, 9(5),
230 689–695.
- 231 20. Mishra, A.; Gairola, R. M.; Varma, A. K. and Agarwal, V. K. 2011b: Improved rainfall estimation over Indian
232 land oceanic regions using satellite infrared technique. *Advances in Space research*, 48: 49-55.
233 doi:10.1016/j.asr.2011.02.016.
- 234 21. Mishra, A.; Gairola, R. M.; Varma, A. K. and Agarwal, V. K. 2010: Remote sensing of Precipitation over
235 Indian land and oceanic regions by synergistic use of multi-satellite sensors. *Journal of Geophysical*
236 *Research*, 115, D08106. doi no. 10.1029/2009JD012157.

- 237
238
239
240
241
242
243
244
245
246
247
248
249
250
251
252
253
254
255
22. Mishra, A.; Gairola, R. M.; Varma, A. K.; Sarkar, A. and Agarwal, V. K. 2009a: Rainfall Retrieval over Indian land and oceanic regions from SSM/I Microwave data. *Advances in Space research*, 44, 815–823.
 23. Mishra, A.K. 2012: Estimation of heavy rainfall during cyclonic storms from microwave observations using nonlinear approach over Indian Ocean. *Natural hazards*, 63(2), 673–683.
 24. Mishra, A. and Rafiq, M., 2017: Towards combining GPM and MFG observations to monitor near real time heavy precipitation at fine scale over India and nearby oceanic regions. *Dynamics of Atmospheres and Oceans*, 80, pp.62–74.
 25. Rafiq, M. and Mishra,A.K. 2017: A study of heavy snowfall in Kashmir, India in January 2017, *Weather*. DOI:10.1002/wea.3065.
 26. Rao, B. D. V.; Hari Prasad, D. and Srinivas, D., 2009: Impact of horizontal resolution and the advantages of the nested domains approach in the prediction of tropical cyclone intensification and movement. *Journal of Geophysical Research*. 114, D11106. doi:10.1029/2008JD011623.
 27. Roca, R.; Viollier, M.; Picon, L. and Desbois, M. 2002: A multisatellite analysis of deep convection and its moist environment over the Indian Ocean during the winter monsoon. *Journal of geophysical research*, 107, (D19). doi:10.1029/2000JD000040.
 28. Rosenfeld, D. and Gutman, G. 1994: Retrieving microphysical properties near the tops of potential rain clouds by multispectral analysis of AVHRR data. *Atmospheric research*, 34(1), 259–283.
 29. Scofield, R. A. and Kuligowski, R. J. 2003: Status and outlook of operational satellite precipitation algorithms for extreme-precipitation events. *Mon. Wea. Rev*, 18,1037–1051.



© 2018 by the authors; licensee MDPI, Basel, Switzerland. This article is an open access article distributed under the terms and conditions of the Creative Commons Attribution (CC-BY) license (<http://creativecommons.org/licenses/by/4.0/>).